JOURNAL OF MATERIALS SCIENCE **34** (1999) 5919–5922

Two limits of melting temperatures of nanocrystals

Q. JIANG, Z. ZHANG
Department of Materials Science and Engineering, Jilin University of Technology, Changchun 130025, People's Republic of China
E-mail: jiangq@post.jut.edu.cn

D. T. HSU, H. Y. TONG, M. ISKANDAR
School of Engineering, University of California, Irvine, CA 92697-2575, USA

It is demonstrated that the melting temperature of nanocrystals embedded in a matrix exhibit two asymptotic limits as the size of the nanocrystal reaches its smallest value. The lower limit of melting temperatures is related to the disappearance of size-dependent entropy of melting and is considered as the lowest glass transition temperature which is located between Kauzmann temperature and glass transition temperature. The upper limit of a nanocrystal embedded in a matrix is determined by the ratio between the bulk melting temperature of the embedded nanocrystal and that of the matrix. The predicted thermodynamic melting temperature range and the lowest glass transition temperature are supported by available experimental evidences.

1. Introduction

The melting temperature of a free-standing nanocrystal is known to decrease as its size decreases [1–8], while a nanocrystal embedded in the matrix can melt below or above the bulk melting temperature [1, 4, 6]. These experimental observations are well explained by a recent model developed on the basis of suppression or intensification of the thermal vibration of atoms on the crystalline surface or interface [1, 2]. However, the possible lower and upper limits of melting temperatures for nanocrystals, which reveal the thermodynamic liquid-crystal transition temperature range, are not clear. The purpose of this contribution is address this issue. It will be demonstrated that the lower limit of melting temperature is related to the disappearance of the size-dependent entropy of melting, and the upper limit of nanocrystals embedded in matrices is determined by the ratio between the bulk melting temperature of the embedded nanocrystal and that of the corresponding matrix. Furthermore, the lower limit is located between Kauzmann temperature and glass transition temperature. These results are of importance for a further understanding of the thermodynamic behavior of nanocrystals and glass transition.

2. Theory

The recent model for size-dependent melting temperature $T_m(r)$ of nanocrystals with a radius of r is given by [1, 2],

$$T_m(r)/T_m(\infty) = \exp[-(\alpha - 1)/(r/r_0 - 1)], \quad (1)$$

where $T_m(\infty)$ is the corresponding bulk melting temperature for $T_m(r)$, α is the ratio between mean-square displacement (msd) of atoms on the surface $\sigma_s^2(r)$ and that within the particle $\sigma_v^2(r)$, r_0 denotes a radius at which all atoms of the nanoparticle are located on the surface,

$$r_0 = (3 - d)h, \quad (2)$$

where h is the atomic diameter in a crystalline lattice and d is the dimension number of low-dimensional crystals [2]. $d = 0$ for nanocrystals, $d = 1$ for crystalline nanowires and $d = 2$ for crystalline thin films [2]. In Equation 1, if $\alpha > 1$, $T_m(r) < T_m(\infty)$. Otherwise, when $\alpha < 1$, $T_m(r) > T_m(\infty)$. As $|\alpha - 1|$ increases, $|T_m(r) - T_m(\infty)|$ increases. Therefore, when the largest value of α (α_{max}) and the smallest value of $\alpha(\alpha_{min})$ can be determined, the lower and the upper limits of $T_m(r)$, T_{min} and T_{max}, are obtained.

Since a crystal is characterized by its long-range order, the smallest nanocrystal should have at least a half of the atoms located within the particle. Hence, the smallest radius of a nanocrystal, r_{min}, is defined as $2r_0$. This definition is supported by experimental evidences. It has been found that when the thickness of a Bi thin film decreases to 0.4 nm, its crystallinity disappears [9]. This observation is expected since for the Bi thin film, $d = 2$ in terms of Equation 2, $h = 0.20$ nm [10] and $2r_0 = 0.40$ nm. For a Pb nanowire in carbon nanotubes, $d = 1$ from Equation 2, $h = 0.39$ nm [10] and $2r_0 = 1.56$ nm, which again is fully consistent with the experimental observation that the crystallinity of Pb disappears at $r = 1.5$ nm [11]. Because $2r_0$ is a critical size where the smallest nanocrystal can exist, the entropy difference between the crystal and liquid or amorphous states below $2r_0$ will disappear, i.e.,

$$s_{lc}(2r_0, T) = 0. \quad (3)$$

Now, we will derive the melting temperature for the smallest free-standing nanocrystal of size $2r_0$, $T_m(2r_0)$. Before doing so, we will first introduce an expression for the size dependence of the entropy of melting for nanocrystals which is related to the lower limit of melting temperature of nanocrystals.

2.1. Lower limit of melting temperature of nanocrystals

According to Mott, vibrational entropy of melting of a bulk crystal, $s_{vib}(\infty)$ is simply determined by its melting temperature $T_m(\infty)$, i.e. [12, 13],

$$s_{vib}(\infty) \propto (3k/2)\ln[T_m(\infty)], \tag{4}$$

As a generation, the size dependence of the vibrational entropy $s_{vib}(r)$ for a nanocrystal can be written as,

$$s_{vib}(r) - s_{vib}(\infty) = (3k/2)\ln[T_m(r)/T_m(\infty)]. \tag{5}$$

Substituting Equation 1 into Equation 5, $s_{vib}(r) = s_{vib}(\infty) - (3k/2)(\alpha - 1)/(r/r_0 - 1)$. Since the entropy of melting for metallic crystals is mainly vibrational in nature [13], one may suggest that $s_m(r)$ for metallic nanocrystals follows the same size dependence as $s_{vib}(r)$,

$$s_m(r) = s_m(\infty) - (3k/2)(\alpha - 1)/(r/r_0 - 1). \tag{6}$$

Since $s_{lc}(2r_0, T) = 0$, i.e., Equation 3, the entropy of melting for a free-standing nanocrystal of size $2r_0$ should also be zero,

$$s_m(2r_0) \equiv s_{lc}[2r_0, T_m(2r_0)], \tag{7}$$

which enables us to obtain an expression for α (for a free-standing nanocrystal, $\alpha = \alpha_{max}$) from Equation 6,

$$\alpha_{max} = 2s_m(\infty)/(3k) + 1. \tag{8}$$

Equation 8 implies that $\alpha_{max} > 1$ since $s_m(\infty) > 0$. In terms of Equation 1 and 8, the melting temperature for the free-standing nanocrystal in a size of $2r_0$ is obtained,

$$T_{min} = T_m(2r_0)_{\alpha>1} = T_m(\infty)\exp[-2s_m(\infty)/(3k)]. \tag{9}$$

It is interesting to point out that as a first-order phase transition, melting degenerates into a continuous second-order transition as the nanocrystal size reaches its limiting value of $2r_0$. This is because T_{min} is a crystal-liquid equilibrium transition temperature, the Gibbs free energy of melting, $g_m(T_{min}) = 0$, and consequently, the enthalpy of melting, $h_m(T_{min}) = 0$. This result that $g_m(T_{min}) = h_m(T_{min}) = s_m(T_{min}) = 0$ is similar to the suggestion by Lam and Okamoto that the crystal-glass enthalpy difference is equal to zero at the highest crystal-glass transition temperature [14].

Because of the above transition characteristics at T_{min}, T_{min} is certainly associated with glass transition temperatures (a second-order transition), i.e., Kauzmann temperature (T_k) and the glass transition temperature (T_g). According to Kauzmann, $s_{lc}(\infty, T_k) = 0$ [15,16]. Since $s_{lc}(r, T)$ decreases as r and T decrease [15], $s_{lc}(\infty, T_{min}) > 0$ or $T_{min} > T_k$. In addition, $s_{lc}(2r_0, T_{min}) = g_{lc}(2r_0, T_{min}) = 0$ at T_{min}, a glass-liquid transition at T_{min} can thermodynamically occur with the smallest size of the liquid in $2r_0$. Thus, T_{min} can be considered as the lowest glass transition temperature which can be obtained only by a zero cooling (or heating) rate without crystallization. Therefore, it is lower than usual measured glass transition temperature, T_g, for instance, by heating a glass with a rate of 20 K min^{-1} on a calorimeter. Hence, there is,

$$T_k < T_{min} < T_g. \tag{10}$$

2.2. Upper limit of melting temperature of nanocrystals

By firmly establishing the lower limit of T_{min} for the melting of a free-standing nanocrystal, we can also show that the melting of a nanocrystal embedded in a matrix has an upper limit. Firstly, we introduce the following relationship [8, 9, 17, 18],

$$\sigma^2(r) \propto T_m(r)/[m\Theta_D(r)^2], \tag{11}$$

where m is the atomic weight and $\Theta_D(r)$ is the size-dependent Debye temperature. With Equation 11, we will analyze the influence of matrices on $\sigma^2(r)$ of embedded nanocrystals. For an embedded nanocrystal in a matrix, its atoms on the surface are no more free-standing. Thus, α could be decreased if there is the interaction on interfaces between the embedded nanocrystal and the matrix [1]. The limit case is that the nanocrystal has a full coherent interface with the matrix and α reaches its smallest value of α_{min}. Hence, the msd of the surface atoms of the nanocrystal could be equal to that of the volume atoms of the matrix, i.e., $\sigma_s^2(r) = \sigma_{vm}^2(\infty)$, where the subscript m denotes the matrix. We assume that msd of volume atoms approaches that of the averaged atoms, there are $\sigma_{vm}^2(\infty) \approx \sigma_m^2(\infty)$ and $\sigma_v^2(r) \approx \sigma^2(r)$. With this assumption and at a $T_m(r)$,

$$\begin{aligned}\alpha_{min} &= \sigma_{vm}^2(\infty)/\sigma_v^2(r) \approx \sigma_m^2(\infty)/\sigma^2(r) \\ &= m\Theta_D^2(r)/m_m\Theta_{Dm}^2(\infty).\end{aligned} \tag{12}$$

On the other side, when Equation 11 is related to different melting temperatures: for the matrix at the bulk melting temperature of the matrix, $T_{mm}(\infty)$, and for the embedded nanocrystal at $T_m(r)$, $\sigma_m^2(\infty)/\sigma^2(r) = 1$ according to Lindemann criterion. Hence, from Equation 11,

$$m\Theta_D^2(r)/m_m\Theta_{Dm}^2(\infty) = T_m(r)/T_{mm}(\infty), \tag{13}$$

where $\Theta_{Dm}^2(\infty)$ is the bulk Debye temperature of the matrix. Substituting Equation 13 to Equation 12,

$\alpha_{\min} = T_m(r)/T_{mm}(\infty)$. Since the lowest $T_m(r)$ is $T_m(\infty)$ with $\alpha < 1$, the limit value of $\alpha_{\min}$ is,

$$\alpha_{\min} \rightarrow T_m(\infty)/T_{mm}(\infty). \quad (14)$$

Note that $\alpha_{\min} > 0$, which is physically meaningful since msd of surface atoms of an embedded nanocrystal in a matrix must be larger than zero. Equation 14 implies well known conditions for superheating of embedded nanocrystals in a matrix that $T_{mm}(\infty) > T_m(\infty)$ and the existence of coherent interfaces between embedded nanocrystals and a matrix. With $\alpha_{\min}$, $T_{\max}$ is calculated by Equation 1 at $r = 2r_0$,

$$\begin{aligned} T_{\max} &= T_m(2r_0)_{\alpha<1} \\ &= T_m(\infty)\ \exp[1 - T_m(\infty)/T_{mm}(\infty)]. \end{aligned} \quad (15)$$

From Equations 8 and 15, the value range of α is $T_m(\infty)/T_{mm}(\infty) < \alpha < 2s_m(\infty)/(3k) + 1$. The corresponding temperature range for a thermodynamic melting is $T_{\min} < T_m(r) < T_{\max}$.

It is noted that although only melting temperature limits of nanocrystals are considered in this paper, melting temperature limits for crystalline nanowires and thin films could also been determined by the above model only with different r_0 being a function of dimension number of d as shown in Equation 2.

3. Results

3.1. Melting temperature limits for indium and lead

Our conclusion for two temperature limits of elements outlined above are supported by experimental observations as shown in Figs 1 to 2 where the theoretical predictions and the experimental results of $\ln[T_m(r)/T_m(\infty)]$ vs. $1/(r/r_0 - 1)$ for indium [1] and lead [3, 4] nanocrystals are plotted. The superheating and depression of melting point of the nanocrystals are located in the indicated range at different r's. The melting temperature of indium nanocrystals (Fig. 1) has reached its lower and upper limits having full coherent interfaces with Al (msd of surface atoms of the embedded indium nanocrystals is as same as that of volume atoms of the matrix) and incoherent interface with Fe (the vibration of surface atoms of the embedded indium nanocrystals is influenced little by the matrix), while size-dependent melting temperature of lead nanocrystals (Fig. 2) are within the two limits showing that they have not full coherent or incoherent interfaces with matrices.

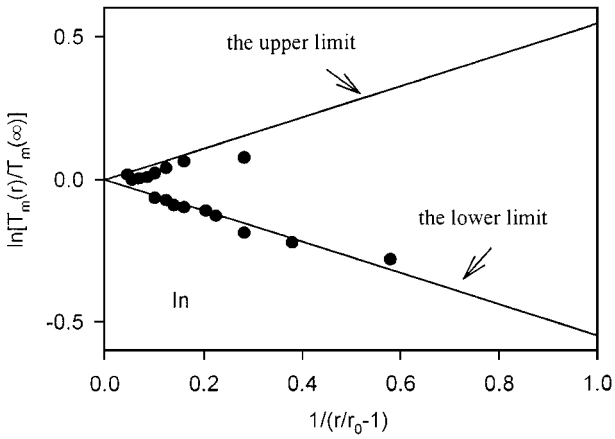

Figure 1 Theoretical prediction of $\ln[T_m(r)/T_m(\infty)]$ vs. $1/(r/r_0 - 1)$ in terms of Equation 1 (solid line) and the corresponding experimental results (●) [1] for indium. The measured results at $T_m(r) < T_m(\infty)$ and $T_m(r) > T_m(\infty)$ are obtained when In nanocrystals are embedded in Fe and Al matrices, respectively. In the figure, h = 0.37 nm [11] and r_0 = 3 h = 1.10 nm. $\alpha_{\min}$ = 0.46 by use of Equation 14 and $\alpha_{\max}$ = 1.55 in terms of Equation 8 with $s_m(\infty)$ = 7.62 Jmol^{-1} K^{-1} [21].

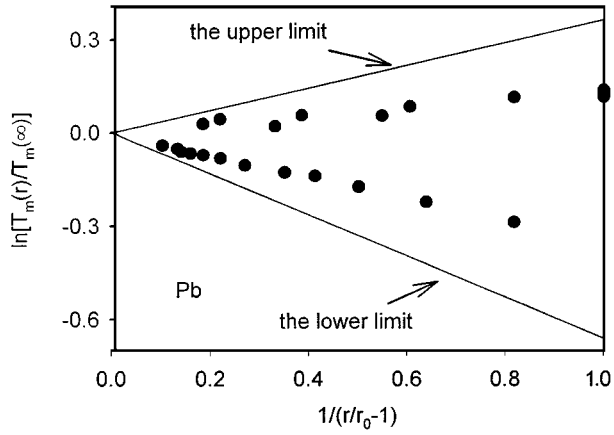

Figure 2 Theoretical prediction of $\ln[T_m(r)/T_m(\infty)]$ vs. $1/(r/r_0 - 1)$ in terms of Equation 1 (solid line) and the corresponding experimental results (●) for lead [3, 4]. In the figure, h = 0.39 nm [11] and r_0 = 3 h = 1.17 nm are used. $\alpha_{\min}$ = 0.64 by use of Equation 14 and $\alpha_{\max}$ = 1.66 in terms of Equation 8 with $s_m(\infty)$ = 8.28 Jmol^{-1} K^{-1} [21].

3.2. Comparison among $T_{\min}$, T_k and T_g

In this section, some experimental results are shown to identify Equation 10. In Table I some predicted values of $T_{\min}/T_m(\infty)$ for metallic elements and that of the calculated $T_k/T_m(\infty)$ based on the specific heat data and Hoch's model [19]. It is clear that $T_{\min} > T_k$ as indicated in Equation 10.

Table II shows the experimental values of $T_g/T_m(\infty)$ of some Fe-, Ni-, Co-, and Pd-based ternary alloys and the prediction of the corresponding $T_{\min}/T_m(\infty)$ with Equation 9. It is clear that $T_{\min} < T_g$ for these glass forming alloys. This result is again in correspondence with Equation 10.

For the most of metallic elements, the values of $s_m(\infty)/k$ are among 0.8 to 1.4, and the corresponding values of $T_{\min}/T(\infty)$ are between 0.4 and 0.6 in

TABLE I Comparison between $T_{\min}/T_m(\infty)$ and $T_k/T_m(\infty)$ for some metallic elements. The data of $T_k/T_m(\infty)$ are cited from [19]

	Li	Na	K	Pb	Sn	In	δ-Fe
$s_m(\infty)/k$	0.80	0.84	0.84	0.96	1.67	0.91	0.92
$T_{\min}/T_m(\infty)$	0.59	0.57	0.57	0.53	0.33	0.54	0.54
$T_k/T_m(\infty)$	0.56	0.54	0.53	0.48	0.26	0.31	0.50

TABLE II Comparison between $T_{min}/T_m(\infty)$ and $T_g/T_m(\infty)$ for some ternary glass forming alloys. The data of $T_g/T_m(\infty)$ are cited from [22]

Alloys(at %)	$s_m(\infty)/k$	$T_{min}/T_m(\infty)$	$T_g/T_m(\infty)$
$Fe_{41.5}Ni_{41.5}P_{17}$	1.49	0.37	0.53
$Co_{75}Si_{15}B_{10}$	1.85	0.29	0.56
$Fe_{79}Si_{10}B_{11}$	1.54	0.36	0.58
$Ni_{75}Si_{18}B_{17}$	1.99	0.27	0.58
$Ni_{65}Pd_{15}P_{20}$	1.74	0.31	0.59
$Fe_{80}P_{13}C_7$	1.97	0.27	0.59
$Pd_{78}Cu_6Si_{16}$	2.21	0.23	0.60
$Pd_{77.5}Cu_6Si_{16.5}$	2.28	0.22	0.64
$Ni_{40}Pd_{40}P_{20}$	1.99	0.27	0.67

terms of Equation 9. However, $T_{min}/T(\infty)$ for ternary glass forming alloys listed in Table II are between 0.2 and 0.4 because the corresponding values of $s_m(\infty)/k$ are among 1.5 to 2.3. Therefore, a strong glass former has a lower T_{min}. It is plausible that the difference between T_g and T_{min} shows the glass forming ability of an alloy. This consideration is meaningful because T_k is only defined for a single element or compound and is unknown for alloys [15].

It should be noted that for binary alloys, a crystallization temperature, T_x, is usually measured to estimate T_g since T_g cannot be obtained by heating a glass on a calorimeter [20]. However, the assumption that $T_x \approx T_g$ is incorrect. Hence, $T_x < T_{min}$ for some binary alloys does not mean that $T_g < T_{min}$.

4. Conclusion

We have provided a microscopic understanding of the lower and the upper limits of the size-dependent melting temperature by introducing the concept of the smallest radius of a nanocrystal. The lower limit is related to the zero entropy of melting in the smallest size of a nanocrystal. The upper limit is related to the ratio of the bulk melting temperature of the embedded nanocrystals and that of the matrix. Two limits are obtained free of any adjustable parameter. According to the model, the thermodynamic melting temperature range is given by $T_{min} < T_m(r) < T_{max}$. Moreover, T_{min} can be considered as the lowest glass transition temperature and $T_k < T_{min} < T_g$. The model is consistent with the available experimental results.

Acknowledgements

Q. J. thanks the support of National Natural Science Foundation of China under Grant No. 59671010 and the helpful discussion with F. G. Shi.

References

1. F. G. SHI, *J. Mater. Res.* **9** (1994) 1307.
2. Q. JIANG, N. AYA and F. G. SHI, *Appl. Phys. A* **64** (1997) 627.
3. V. R. SKRIPOV, V. P. KOVERDA and V. N. SKOKOV, *Phys. Stat. Sol. (A)* **66** (1981) 109.
4. H. H. ANDERSEN and E. JOHNSON, *Phys. Res. B* **106** (1995) 480; K. K. BOURDELLE, A. JOHANSEN, E. JOHNSON and L. SARHOLT-KRISTENSEN, *Mater. Sci. Forum* **179–181** (1995) 659; N. B. THOFT, J. BOHR, B. BURAS, E. JOHNSON and A. JOHANSEN, *J. Phys. D* **28** (1995) 539; G. DYBKJAER, N. KRUSE, A. JOHANSEN, E. JOHNSON, L. SARHOLT-KRISTENSEN and K. K. BOURDELLE, *Surf. Coating Tech.* **83** (1996) 82; K. K. BOURDELLE, A. JOHANSEN and E. JOHNSON, *Phys. Res. B* **118** (1996) 478.
5. A. N. GOLDSTEIN, *Appl. Phys. A* **62** (1996) 33.
6. H. W. SHENG, G. REN, L. M. PENG, Z. Q. HU and K. LU, *J. Mater. Res.* **12** (1997) 119.
7. S. L. LAI, J. Y. GUO, V. PETROVA, G. RAMANATH and L. H. ALLEN, *Phys. Rev. Lett.* **77** (1996) 99.
8. J. R. CHILDRESS, C. L. CHIEN, M. Y. ZHOU and P. SHENG, *Phys. Rev. B* **44** (1991) 11 689.
9. M. G. MITCH, S. J. CHASE, J. FORTNER, R. Q. YU and J. S. LANNIN, *Phys. Rev. Lett.* **67** (1991) 875.
10. H. W. KING, in "Physical Metallurgy", edited by R. W. CAHN (North-Holland Publishing, 1970) p. 60.
11. S. IIJIMA, *Nature* **354** (1991) 56; P. M. AJAYAN and S. IIJIMA, *Nature* **361** (1993) 233.
12. N. F. MOTT, *Proc. R. Soc. A* **146** (1934) 465.
13. A. R. REGEL', V. M. GLAZOV, *Semiconductors* **29**(5) (1995) 405.
14. N. Q. LAM and P. R. OKAMOTO, MRS Bulletin **19** (7) (1994) 41.
15. W. KAUZMANN, *Chem. Rev.* **43** (1948) 219.
16. F. G. SHI, *J. Mater. Res.* **9** (1994) 1908.
17. V. K. MALINOVSKY, V. N. NOVIKOV, *J. Phys.: Condens. Matter* **4** (1992) L139.
18. Q. JIANG, H. Y. TONG, D. T. HSU, K. OKUYAMA and F. G. SHI, *Thin Solid Film* **312** (1998) 357.
19. M. HOCH, *Metall. Trans.* **23B** (1992) 309.
20. R. LÜCK, Q. JIANG and B. PREDEL, *J. Non-Cryst. Solids.* **117–118** (1990) 911.
21. A. R. UBBELHDE, "The Molten State of Matter" (John-Wiley & Sons, 1978) p. 238–241.
22. K. LU, *Acta Metall. Sin.* **28** (1992) B17.

Received 12 August 1997
and accepted 18 May 1999